Magnesium Technology 2013
Edited by: Norbert Hort, Suveen N. Mathaudhu, Neale R. Neelameggham, and Martyn Alderman
TMS (The Minerals, Metals & Materials Society), 2013

Effect of Casting Defects Distribution on the Beginning of Tensile Fracture in Semi-solid Injected Magnesium AZ91D Alloy

Yuichiro Murakami[1], Kenji Miwa[2], Naoyuki Kanetake[3], Shuji Tada[1]
[1]Materials Research Institute for Sustainable Development, National Institute of Advanced Industrial Science and Technology (AIST); 2266-98, Anagahora, Shimo-Shidami, Moriyama-ku; Nagoya, Aichi, 463-8560, Japan
[2]Aichi Science and Technology Foundation; 1-157-1, Onda-cho; Kariya, Aichi, 448-0013, Japan
[3]Nagoya University; Furo-cho, Chikusa-ku; Nagoya, Aichi, 464-8603, Japan

Keywords: Semi-soid injection process, Magnesium alloy, Tensile fracture, Casting defects, X-ray CT

Abstract

Semi-solid process is useful for magnesium alloys because processing temperatures lower than conventional casting processes result in decreased combustibility. Additionally it can decrease casting defects by the increased viscosity and decreased solidification shrinkage. In this study, casting defects of semi-solid injected AZ91D specimens were observed by X-ray CT tomography and tensile test was carried out. Thus, relations between casting defects and fracture starting point were investigated. As a result, the specimens were not always fractured at the site of the largest defect; meanwhile the defects situated near the surface or perpendicularly elongated to the tension axis exerted a potent influence on fracture.

Introduction

In recent years, global warming and global climate change have recently become an international concern. Hence the development of environmental protection programs and green technology is becoming considerably important. To solve these issues, the reduction of carbon dioxide emissions and improvement of fuel efficiency are urgent issues for the transportation machine. In particular, the reduction of vehicle weight is highly effective means of improving fuel efficiency and it has a positive impact for reduction of CO_2 emissions from transport. The expanded use of light metals such as aluminum and magnesium is considered one of the most effective methods for reducing vehicle weight. Magnesium in particular is considered to be a promising lightweight structural material because it has excellent specific strength, and has the lowest density among applicable metallic materials.

The die-casting process is among the most commonly used methods for forming magnesium alloy products with complex configurations. However, products molded by die-casting exhibit low engineering performance due to the existence of inherent defect such as porosity, hot cracks and oxide inclusions. Additionally, die-casting of magnesium alloys requires the use of cover gas because magnesium alloys are easy combustible in the liquid state.

The semi-solid forming process is a near net shape variant of die casting, which is carried out at the solid-liquid co-existence phase, which was first developed in the early 1970s [1, 2]. Recently, this process has been applied to fabricate high-quality aluminum alloy [3-5] or magnesium alloy products [6-8]. The semi-solid forming process uses semi-solid slurry that has a higher viscosity and smaller liquid fraction than liquid metal; hence this process is expected to reduce casting defects in the final components. Additionally this process is considered useful for magnesium alloys because processing temperatures lower than conventional casting processes result in decreased combustibility of the magnesium alloy.

We have developed a new type of semi-solid injection process that allows magnesium alloys form in high material yield [9-12]. In this process, magnesium billets are heated to the semi-solid temperature range in an injection cylinder. Thus, the semi-solid magnesium alloy is not exposed to air, so this process requires no cover gas. Also particular billet is used in the semi-solid injection process in general because the billet cannot have fluidity even if the commercial billet is heated to the semi-solid temperature. On the other hand, the fluidity of the semi-solid slurry can be improved by applying shear stress [13]. In our new process, shear stress is applied to the slurry before injecting into the mold. Therefore commercial magnesium billets can be used.

On the other hand, the semi-solid products differ in character from conventional castings. For example, the distribution of the primary Mg particles was not uniform in the thickness direction [11], and mechanical strength was affected by not only casting defects but also fraction solid [12]. In this study, plate specimens were made by using a testing machine implementing the proposed semi-solid injection method, after which tension test was carried out. The effects of distribution of casting defects on the fracture behavior were investigated.

Experimental procedure

The semi-solid samples were prepared by using the vertical injection system shown in Fig. 1. The injection cylinder is able to heat the magnesium alloy billets to the semi-solid temperature, as well as to maintain this temperature. The injection cylinder in the apparatus was constantly filled with billet to a height of 320 mm under the nozzle, and the billet in the uppermost part of the cylinder was heated to a given semi-solid temperature. The semi-solid billet can then be injected into a permanent mold by a piston. The injection cylinder has an inner diameter of 25 mm, an outer diameter of 60 mm and a length of 54 mm; the nozzle is 3 mm in diameter. The injection cylinder is equipped with six heaters on the surface of the outer wall; these heaters can control the temperature of the billet precisely. The six heaters are controlled independently on the basis of measurements from six thermocouples (H1 to H6), each of which is inserted at the location of a heater. The temperature of the billet in the uppermost part of the injection cylinder (from the nozzle to a height of 130 mm) was controlled within ±1 °C by setting the temperature of H1 (from the nozzle to a height of 21 mm) and H2 (from the nozzle to a height of 151 mm). The temperature of the billet in the uppermost part of the injection cylinder (from the nozzle to 130 mm height) was set to the temperature in the semi-solid range, namely, 591 °C or 586 °C. The fraction solid f_s was 0.3 or 0.4, respectively, at each of these temperatures. On the other hand, the

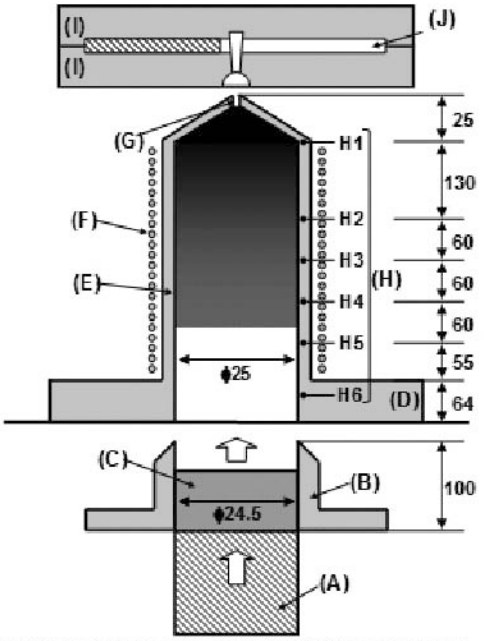

Fig. 1 Schematic representation of semi-solid forming apparatus

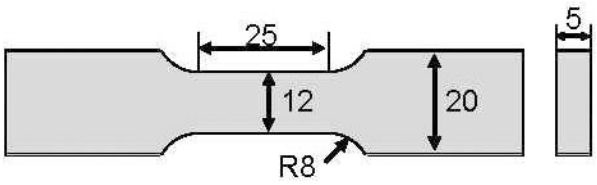

Fig. 2 Schematic image of tensile test piece

temperature of the billet closer to the bottom was decreased by controlling the temperature of heaters H3 to H6, and billet at the bottom was in a solid state. There is not much risk of combustion in a system with such design since billet in the semi-solid state is not exposed to air. Therefore, this experiment was carried out in air, without the use of a cover gas or inert gas.

The permanent mold in the experiment was a plate cavity of 20 mm in width, 100 mm in length and 5 mm in thickness. The slurry was injected horizontally since the mold was mounted vertically, and the mold clamping force was set to 274.4 kN. The amount of injected slurry per cycle was about 30 g, which was equivalent to the amount of material from the nozzle to a height of 53 mm. The injection speed V, which was calculated from the average piston speed, was set to 400 mm/s. The flow speed of the slurry at the nozzle was 27.8 m/s at each of these injection speeds.

The microstructures of these specimens were observed by optical microscopy. The samples were molded in epoxy resin and polished by grinding with SiC paper, followed by polishing with diamond paste, then, the specimens were etched in a solution of 75 ml ethylene glycol, 1 ml nitric acid and 24 ml distilled water. The plate specimens were mechanically processed into tensile test pieces shown as Fig. 2. Each tensile test piece was 100 mm in length, 20 mm in width 25 mm in gage length, 5 mm in thickness and 8 mm in shoulder radius. In addition, the surface of the test piece was as cast. Tensile tests were carried out at the room temperature by applying tension at a speed of 1.0 mm/s to 4 samples per set of casting conditions.

Also, distribution of casting defects in the specimens were analyzed on an X-ray computerized tomography (CT) scanner before and after tensile test. The rendered images were created from cross-sectional images obtained with 3D rendering software (VGStudio Max 2.0, Volume Graphics Inc.). In addition, the resolution of X-ray CT was 46 μm, allowing for detection of casting defects greater than 8 voxels.

Results and discussion

Microstructure of specimen and distribution of α-Mg particles

Fig. 3 shows a typical microstructure at the plane perpendicular to the slurry flow direction. The observation point was 50 mm from the gate. These micrographs show that the specimen has a homogeneous microstructure with a uniform dispersion of primary α-Mg in the matrix (eutectic α-Mg and β-$Mg_{17}Al_{12}$). When the slurry was injected, the solid phase consisted of the α-Mg particles with the matrix as the liquid phase. The distribution of the solid particles in the thickness direction was nonuniform. The solid particles have a tendency to concentrate in the center of the plate for all conditions. Additionally, the density of the solid particles at the surface was low, and, especially at a fraction solid of 0.3, the surface was nearly devoid of solid particles.

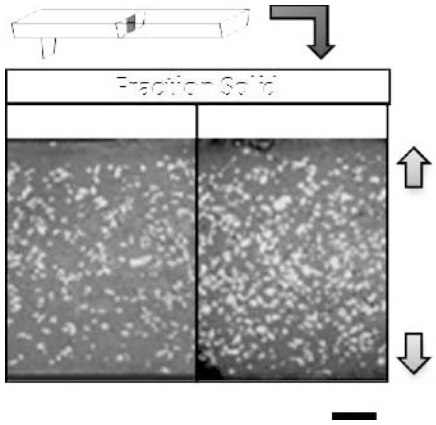

Fig. 3 Optical micrographs of the center of the specimen in the plane perpendicular to the flow direction.

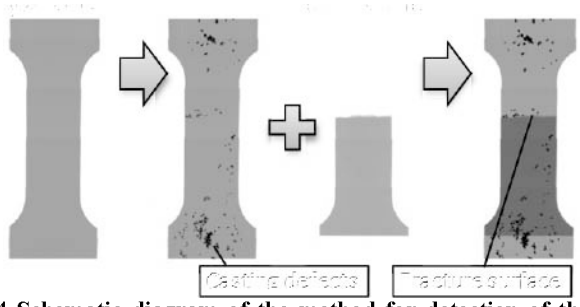

Fig. 4 Schematic diagram of the method for detection of the fracture surface.

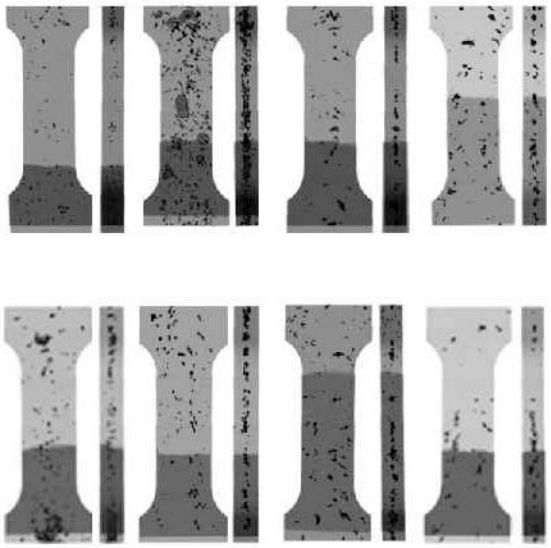

Fig. 5 Results of fracture surface detection and relation between distribution of casting defects and fracture surface.

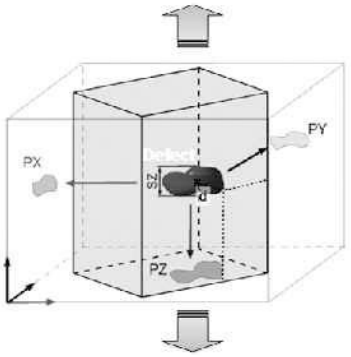

Fig. 6 Schematic view of the parameters for calculating indexes.

Fracture surface detection by X-ray CT

Detection of the fracture surface was carried out in the following way. First, the samples were scanned by X-ray CT before and after tensile test, as shown in Fig. 4. A 3D image of the sample before the tensile test was rendered by X-ray CT data, and casting defects in the sample were detected by contrast difference in the rendering image. Next, a rendering image of the sample after the tensile test was made from X-ray CT data. After that, this image was superimposed on the rendering image before the tensile test, thus the fracture surface was appeared. Additionally, casting defects involved in the fracture could be detected.

Fig. 5 shows results of fracture surface detection and relation between distribution of casting defects and fracture surface. Weiler et al. [14] showed the areal fraction of defects appeared to be the major factor in the fracture of the tensile test at magnesium high pressure die-cast samples. In this study, some samples fractured at the largest point of the areal fraction of defects (e.g., sample (a)-2). On the other hand, many samples were not always

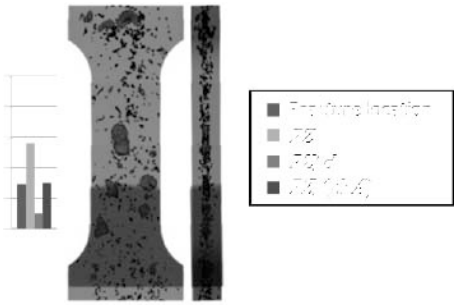

Fig. 7 Comparison of the sample (a)-2 with the maximum point of calculated indexes PZ, PZ/d, and PZ/(d・F).

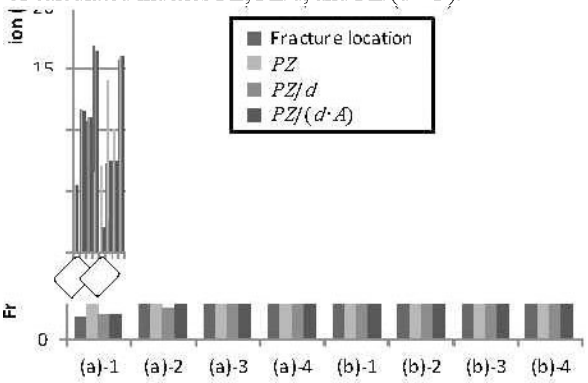

Fig. 8 Relation between the fracture location of samples and the maximum point of calculated indexes *PZ*, *PZ/d*, and *PZ/(d·F)*. The fracture surface location was measured as a distance from the bottom of the gage.

fractured at the largest point of cross sectional areal fraction of defects.

Relation between fracture surface and casting defects

From preceding section, the cross sectional area *PZ*, distance from the surface *d* and shape of casting defects are thought to have effects on fracture. There, we calculated two indexes to clarify the factor of fracture of semi-solid materials. Schematic view of the parameters for calculating indexes was shown in Fig. 6. First one was *PZ/d*, where *PZ* is cross sectional area of casting defects projected on the plane perpendicular to the tensile axis, and *d* is distance from surface. This index includes the effect of distance from the surface, then this index becomes greater if the defect is located near the surface. Second one was *PZ/(d·F)*, where *F* is described as follows.

$$F_x = SZ/\left(2\sqrt{\frac{PX}{\pi}}\right), F_y = SZ/\left(2\sqrt{\frac{PY}{\pi}}\right)$$

where, *SZ* is the length of the tensile axis direction of a defect, *PX* and *PY* are projected areas of perpendicular to the tensile axis. Then, if $F_x \geqq F_y$, $F = F_y$, else if $F_x < F_y$, $F = F_z$. If a defect has oblate shape and expands to perpendicular to the tensile axis, this parameter becomes small. Thus, the index *PZ/(d·F)* includes the effect of both the location and size effect of casting defect. Fig.7 shows the comparison of sample (a)-2 with the maximum point of calculated indexes PZ, PZ/d, and PZ/(d・F). By this comparison, it is made clear that this sample was fractured at the largest PZ/(d・F).

Fig. 8 shows comparison between the fracture location of samples and the maximum point of calculated indexes. The vertical axis in Fig. 8 shows the location of the fracture which was measured as a percentage of the entire gage length from the bottom of the gage. Only sample (a)-4 fractured at the largest *PZ*. On the other hand, the samples fractured at the largest PZ/d were 6 of 8. This result means that the fracture of semi-solid metal is affected by not only cross sectional area of casting defects but also site of casting defect. That is the casting defect located near surface has the large impact on fracture. Furthermore, all samples but (b)-3 were fractured at the largest $PZ/(d \cdot F)$. Therefore, the casting defects with flat perpendicular to the tensile axis shape are thought to have larger impact on fracture.

These different results from die-casting [15] are thought to be after effects of not uniform structure. Such as the primary α-Mg particles have a tendency to concentrate in the center of the plate and the density of the primary α-Mg particles at the surface was low. In the semi-solid magnesium AZ91D, a hardness of the matrix (eutectic α-Mg and β-$Mg_{17}Al_{12}$) is greater than primary α-Mg particles. The defect near the surface is thought to be located at the high strength matrix. Thus the lack of matrix which can shoulder high stress is thought to be reason that the casting defect located near surface has the large impact on fracture. Then the casting defects with the shape like flat perpendicular to the tensile axis have the large impact on fracture. This is considered the effect of stress concentration on the sharp edge of defects perpendicular to the tensile axis.

Conclusions

To investigate the effect of the distribution of casting defects on the fracture, X-ray CT scanning and tensile test of the AZ91D magnesium specimens made by the semi-solid injection testing machine were performed. The fracture surface was appeared by the X-ray CT image then the casting defects involved in the fracture could be detected. In this study, the samples were not always fractured at the site of the largest cross sectional areal fraction of casting defects.

Therefore, the two indexes were calculated. One was PZ/d which includes the effect of location, another was $PZ/(d \cdot F)$ which also includes the effect of shape of casting defects. By comparison between the fracture location of samples and calculated indexes, the fracture of semi-solid metal product is appeared to be affected by not only cross sectional area of casting defects but also site and shape of casting defect. That is the casting defect located near surface has the large impact on fracture. Furthermore the casting defects with the shape like flat perpendicular to the tensile axis are thought to more largely affect fracture.

References

1. M.C Flemings and R. Meharabian, "Casting Semi-solid Metals," *AFS Transactions*, 102 (1973), 81-88.

2 . M.C Flemings, "Solidification processing," *Metallurgical and Materials Transaction*, 5B (1974), 2121-2134

3. W.G. Cho and C.G. Kang, "Mechanical properties and their microstructure evaluation in the thixoforming process of semi-solid aluminum alloys," *Journal of Materials Processing Technology*, 105 (2000), 269-277

4. S. Nafisi and R. Ghomashchi, "Grain refining of conventional and semi-solid A356 Al–Si alloy," *Journal of Materials Processing Technology*, 174 (2006), 371-383

5. H.K. Jung and C.G. Kang, "Induction heating process of an Al–Si aluminum alloy for semi-solid die casting and its resulting microstructure," *Journal of Materials Processing Technology*, 174 (2006), 355-364

6. T. Tsukeda, K. Saito, "Mechanical Properties of AM -Series Magnesium Alloy Made by Injection Molding Process" Journal of Japan Foundry Engineering Society, 70 (1998), 697-701 (in Japanese)

7. Z. Koren, H. Rosenson, E.M Gutman, Ya. B. Unigovski, A Eliezer, "Development of semi-solid casting for AZ91 and AM50 magnesium alloys", *Journal of Light Metals*, 2 (2002) 81-87

8 . F. Czerwinski, "Size evolution of the unmelted phase during injection molding of semi-solid magnesium alloys", *Scripta Materialia*, 48 (2003), 327-331

9. N. Omura, Y. Murakami, M.G. LI, T. Tamura, K. Miwa, "Effect of Volume Fraction Solid and Injection Speed on Mechanical Properties in New Type Semi-solid Injection Process," *Solid State Phenomena*, 141-143 (2008) 761-766

10. Y. Murakami, N. Omura, M.G. Li, T. Tamura, S. Tada, K. Miwa "Microstructures and Casting Defects of Magnesium Alloy Made by a New Type of Semi-solid Injection Process," *Magnesium Technology 2011*, (2011) 107-112

11. Y. Murakami, N. Omura, M. Li, T. Tamura, K. Miwa, "Effect of Injection Speed on Microstructure of AZ91D Magnesium Alloy in Semi-solid Injection Process", *Materials Transactions*, 53 (2012), 1094-1099

12 . Murakami, K. Miwa, N. Omura, S. Tada, "Effects of Injection Speed and Fraction Solid on Tensile Strength in Semi-solid Injection Molding of AZ91D Magnesium Alloy", *Materials Transactions*, 53 (2012), in press

13. Y. Murakami, K. Miwa, M, Kito, T. Honda, N. Kanetake, S. Tada, "Effect of Injection Conditions in Semi-solid Injection Process on Fluidity of AC4CH Aluminum Alloy", *Journal of Japan Foundry Engineering Society*, 84 (2012), in press

14. J.P. Weiler, J.T. Wood, R.J. Klassen, E. Maire, R. Berkmortel, G. Wang, "Relationship between internal porosity and fracture strength of die-cast magnesium AM60B alloy", *Materials Science and Engineering A*, 395 (2005), 315-322

15. J.P. Weiler, J.T. Wood, R.J. Klassen, E. Maire, R. Berkmortel, G. Wang, "Relationship between internal porosity and fracture strength of die-cast magnesium AM60B alloy", *Materials Science and Engineering A*, 395 (2005), 315-322